

Electronic Supplementary Information for

Ionic liquid decoration for hole transport improvement of PEDOT

Wei-Lu Ding^a, Xing-Liang Peng^b, Zhu-Zhu Sun^c, Kailun Bi^{a,d}, Yaqin Zhang^a, Yanlei Wang^a, Lin Ji^d, and Hongyan He^{*a}

^a Beijing Key Laboratory of Ionic Liquids Clean Process, CAS Key Laboratory of Green Process and Engineering, State Key Laboratory of Multiphase Complex Systems, Institute of Process Engineering, Chinese Academy of Sciences, Beijing 100190, People's Republic of China

^b MOE Key Laboratory of Organic OptoElectronics and Molecular Engineering, Department of Chemistry, Tsinghua University, Beijing 100084, People's Republic of China

^c Energy-Saving Building Materials Innovative Collaboration Center of Henan Province, Xinyang Normal University, Xinyang, 464000, People's Republic of China

^d Department of Chemistry, Capital Normal University, Beijing 100048, People's Republic of China

Corresponding Author:

Email: hyhe@ipe.ac.cn

Contents

Newns–Anderson model	S3
The calculation of reorganization energy	S4
The calculation of hole mobility	S5
Fig. S1. The HOMO and LUMO orbitals of series of cations.....	S6
Fig. S2. The C2 site of imidazolium ring and the configurations of IL-PEDOT interface.....	S7
Fig. S3. Electrostatic potential (ESP) distribution.....	S8
Fig. S4. Dynamic evolution of hole mobility of PEDOT after modulated by [BMIM]:[BF ₄] and [BuPhIM]:[BF ₄]	S9
Fig. S5. IL involved transition orbitals during excitation	S10
Fig. S6. The last snapshots of PEDOT in [BnPhIM- <i>o</i> OMe] ⁺ , [BnPhIM- <i>m</i> OMe] ⁺ , and [BnPhIM- <i>p</i> OMe] ⁺ combined with [BF ₄] ⁻ and [B(CN) ₄] ⁻ modified solution.....	S11
Fig. S7. The distribution of the angle and the $d_{\pi-\pi}$ in PEDOT chains for [BnPhIM- <i>p</i> OCH ₃]:[B(CN) ₄]-PEDOT.....	S12
Fig. S8. The density of states and Lorentzian distribution.	S13
Fig. S9. Dynamic evolution of hole mobility of PEDOT after modulated by [BnPhIM- <i>p</i> OMe]:[B(CN) ₄].....	S14

1 Newns–Anderson model^{1,2}

To explain the interfacial coupling, Newns–Anderson approach was employed to compute the hybridization of the highest occupied molecular orbital (HOMO) on ionic liquid with the manifold occupied orbitals on PEDOT. Accordingly, this hybridization possesses a Lorentzian distribution:

$$\rho(E) = \frac{1}{(\varepsilon_i - E_{\text{H(IL)}})^2 + (\frac{\hbar\Gamma}{2})^2}$$

where ε_i , $E_{\text{H(IL)}}$, and $\hbar\Gamma$ in denominator separately describes i th molecular orbital (MO) energy in the IL-PEDOT complexes, the HOMO energy of IL after coupling with PEDOT, and the broadening width taken as the mean deviation of the HOMO levels of IL and it can be viewed as a critical item to illustrate the hybridization quantitatively. Accordingly, the $E_{\text{H(IL)}}$ and $\hbar\Gamma$ are defined as follows:²

$$E_{\text{H(IL)}} = \sum_i p_i \varepsilon_i$$
$$\hbar\Gamma = \sum_i p_i |\varepsilon_i - E_{\text{H(IL)}}|$$

where p_i is the portion of i th MO for IL, and it is evaluated by:

$$p_i = \frac{\sum_j^{A \in \text{IL}} (c_{ij}^A)^2}{\sum_j^{A \in \text{IL-PEDOT}} (c_{ij}^A)^2}$$

The calculation of reorganization energy (λ)

The reorganization energy (λ) is related to the energy change with the geometry relaxation during charge transport, which can be evaluated by the adiabatic potential energy surface method (the four-point method) and normal mode analysis. The former is expressed as:³

$$\lambda = \lambda_1 + \lambda_2 = (E_+^0 - E_0) + (E_0^+ - E_+^+)$$

where E_+^0 is the energy of the neutral molecule calculated on top of the optimized cationic state, E_0 is the energy of the optimized neutral molecule at ground state, E_0^+ is the energy of the cation calculated on top of the optimized neutral state, and E_+^+ is the energy of the optimized cation, respectively.

And the normal mode analysis assigns the λ to the contribution from each vibrational mode:⁴

$$\lambda = \lambda_1 + \lambda_2 = \sum_i \lambda_{1i} + \sum_j \lambda_{2j} = \sum_i \frac{1}{2} \omega_i \Delta Q_i^2 + \sum_j \frac{1}{2} \omega_j \Delta Q_j^2$$

where λ_{1i} and λ_{2j} stand for the contributions to the λ from vibrational modes i and j of the neutral and cationic geometries separately, ω_i and ω_j represent for the vibrational frequencies of modes i and j , and ΔQ_i and ΔQ_j are the displacements along the i th and j th mode coordinates between the equilibrium positions of neutral and cationic states, respectively. By contrast to the V_{ij} , a minimized λ potentially ensures a large k_{ij} . And in this work, we used these two methods to calculate λ separately.

The calculation of hole mobility

The hole mobility (μ) can be obtained based on the non-adiabatic Marcus charge transfer theory:⁵⁻⁷

$$k_n = \frac{2\pi}{\hbar} |V_{ij}|^2 \sqrt{\frac{1}{4\pi k_B T \lambda}} \exp\left[-\frac{(\Delta G_{ij} + \lambda)^2}{4\lambda k_B T}\right]$$

where \hbar is reduced Planck's constant, V_{ij} is the transfer integral, k_B is Boltzmann's constant, T is temperature in Kelvin, λ is the reorganization energy, and ΔG_{ij} is the energy difference in sites i and j , respectively. Accordingly, the hole mobility (μ) is estimated by Einstein equation:⁸

$$\mu = \frac{eD}{k_B T}$$

$$D = \frac{1}{2d} \sum_n r_n^2 k_n p_n$$

where e and D in numerator represent for the unit charge and diffusion coefficient. Correspondingly, to calculate D , a spatial dimensionality d should be defined (here taken as 1 for amorphous morphology), and associated centroid to centroid distance (r_n), k_n , as well as the hopping probability for the n th hopping pathway ($p_n = k_n / \sum_n k_n$) should be as the input to obtain the diffusion coefficient.

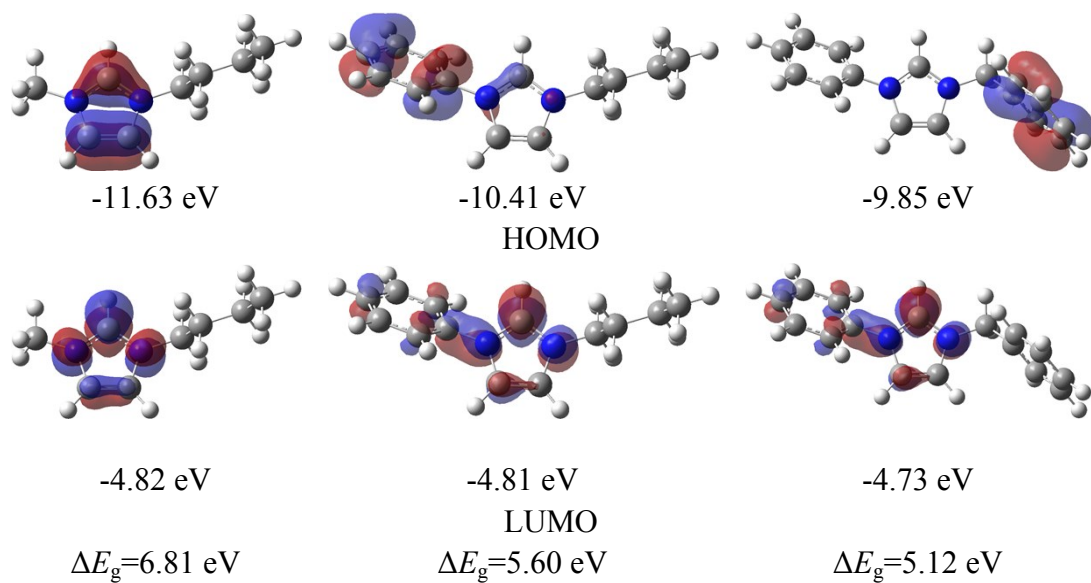
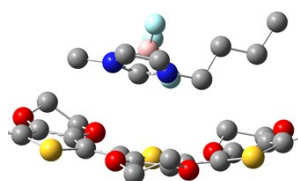
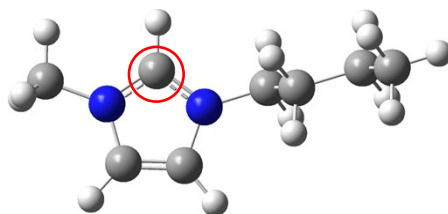
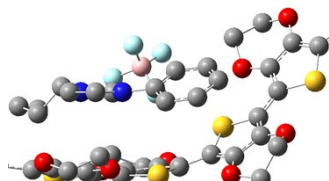


Fig. S1. The HOMO and LUMO orbitals of series of cations (the ΔE_g represents for the energy gap between the HOMO and LUMO).

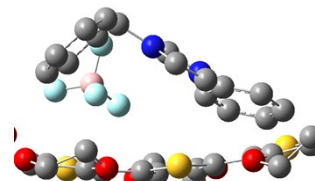
C2 site



[BMIM]:[BF₄]-PEDOT



[BuPhIM]:[BF₄]-PEDOT



[BnPhIM]:[BF₄]-PEDOT

Fig. S2. The C2 site of imidazolium ring and the configurations of IL-PEDOT interface (only the interface of IL-PEDOT complexes has been plotted).

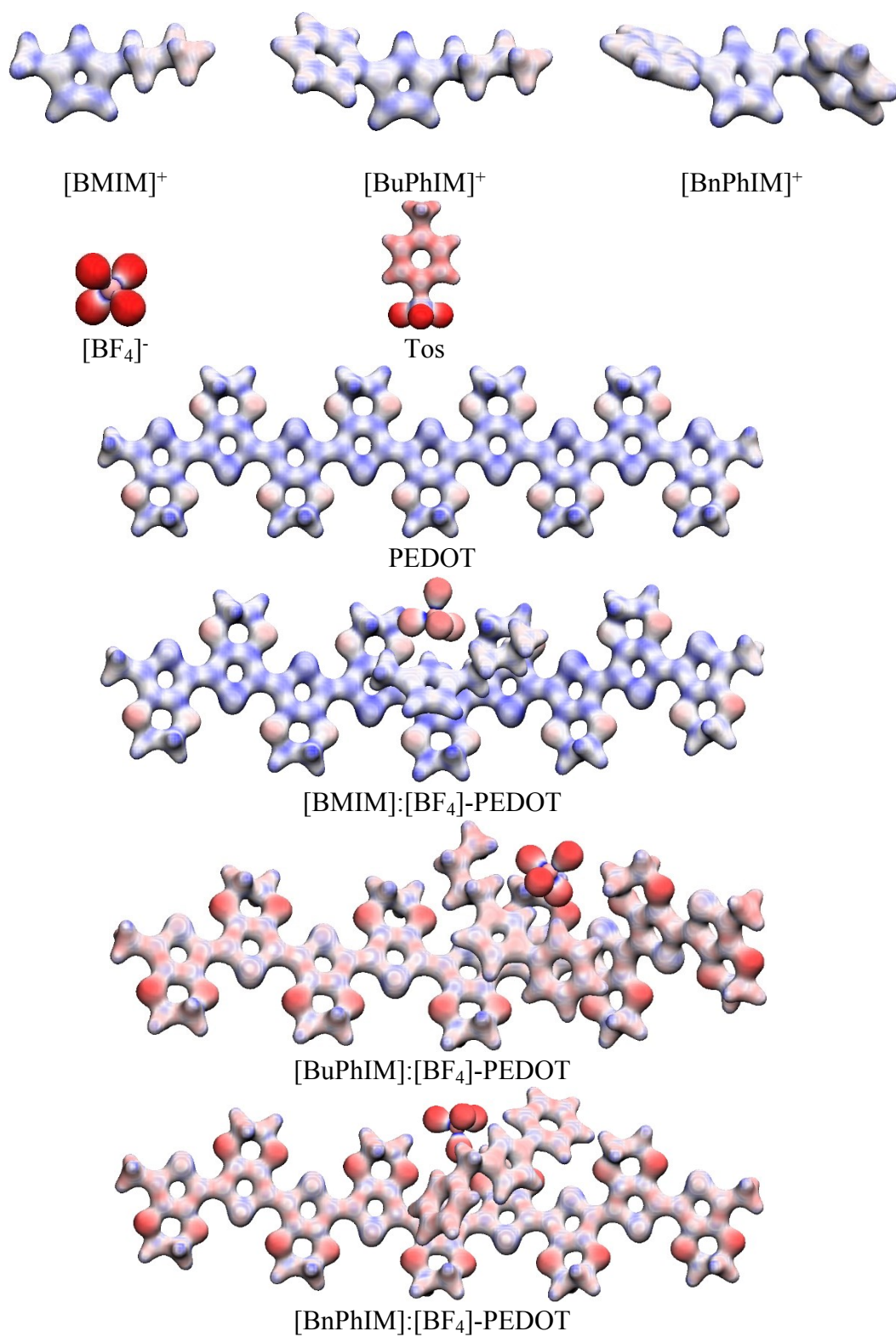
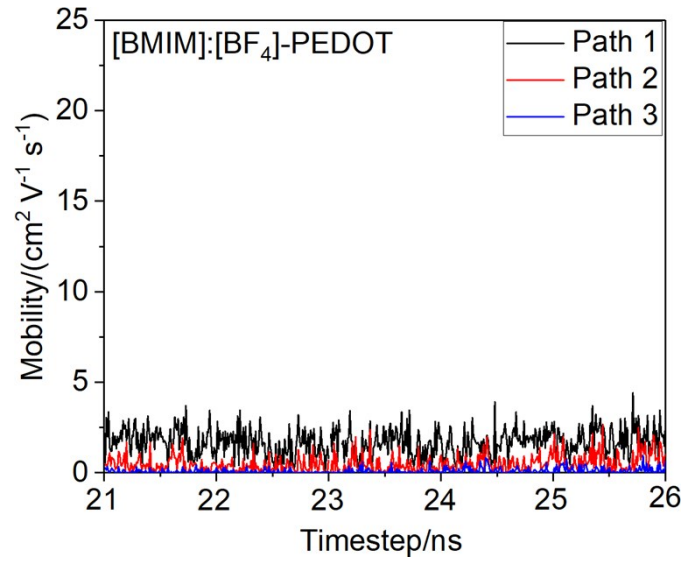
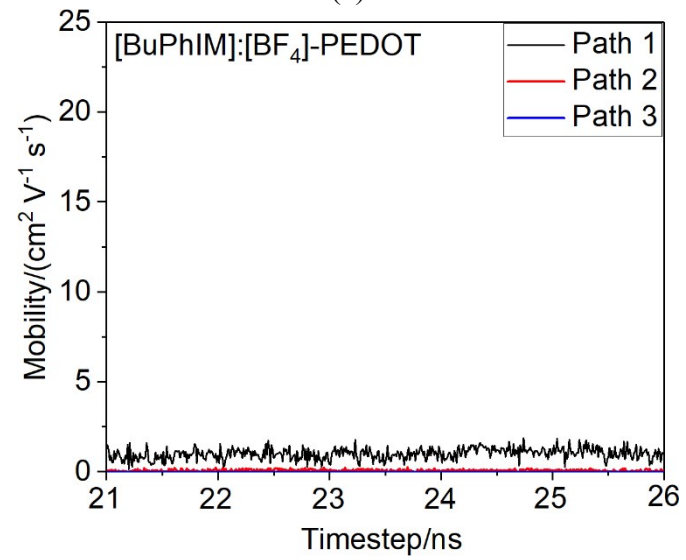


Fig. S3. Electrostatic potential (ESP) distribution mapped onto a surface of total electrons for different components (Isovalue=0.1 a.u.).



(a)



(b)

Fig. S4. Dynamic evolution of hole mobility of PEDOT after modulated by (a) [BMIM]:[BF₄] and (b) [BuPhIM]:[BF₄], respectively.

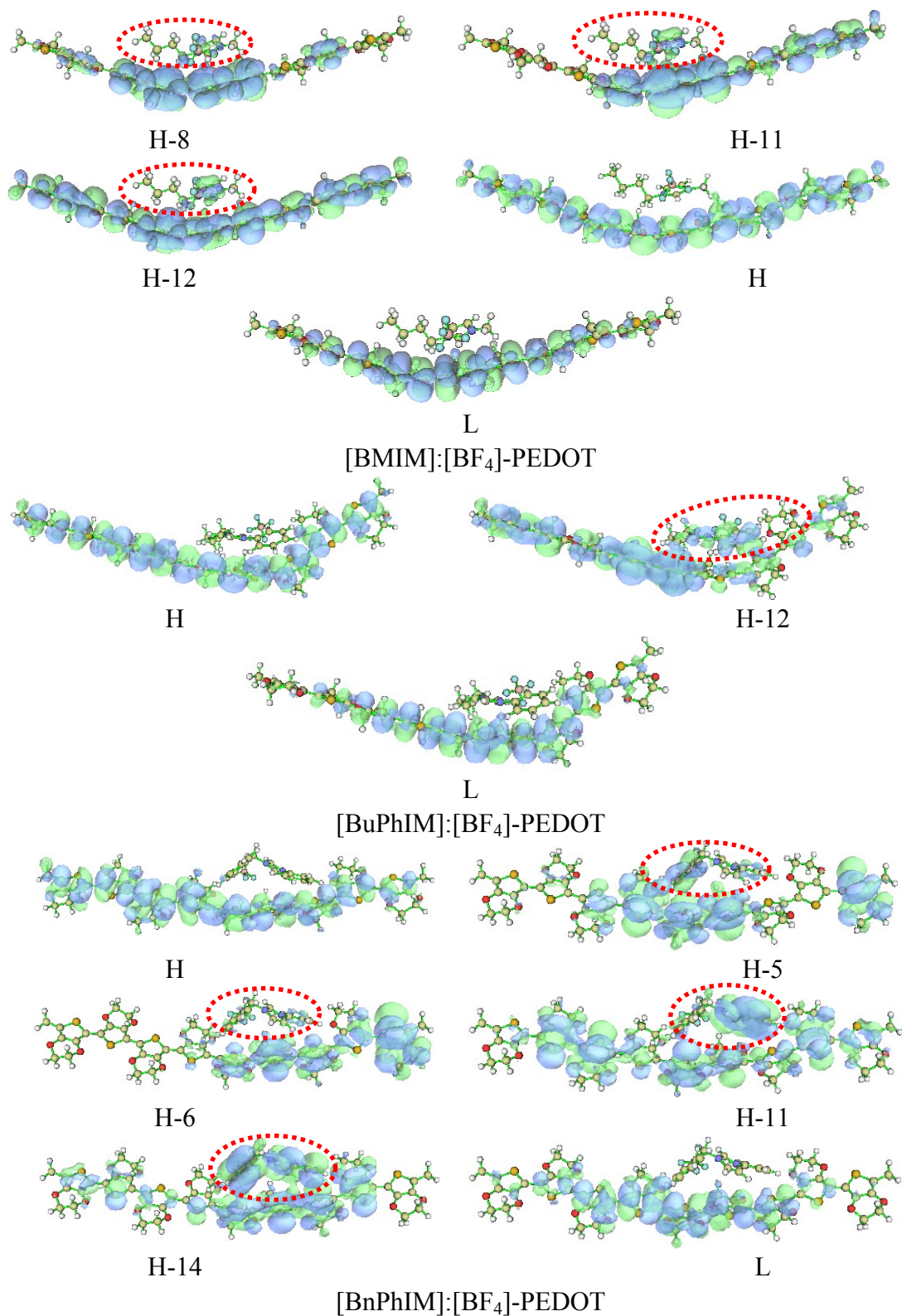
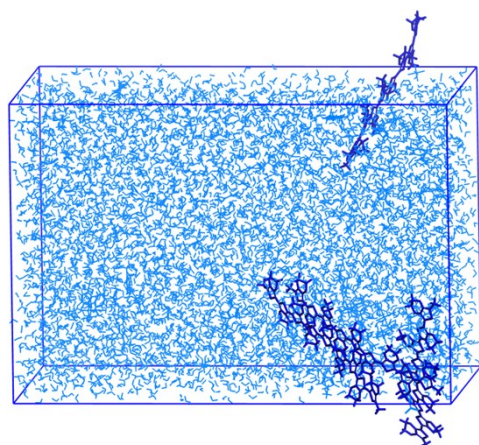
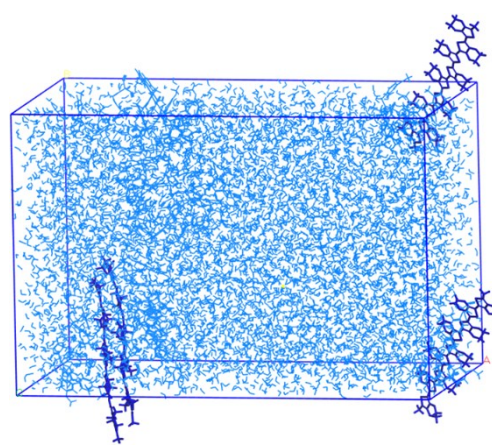


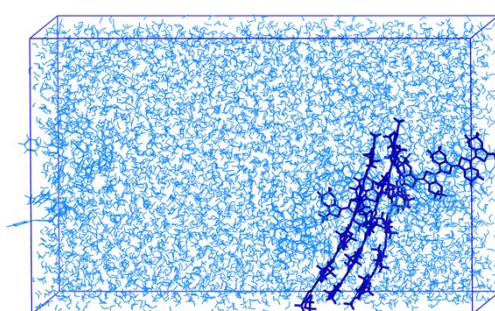
Fig. S5. IL involved transition orbitals during excitation (H and L represent for the HOMO and LUMO, respectively).



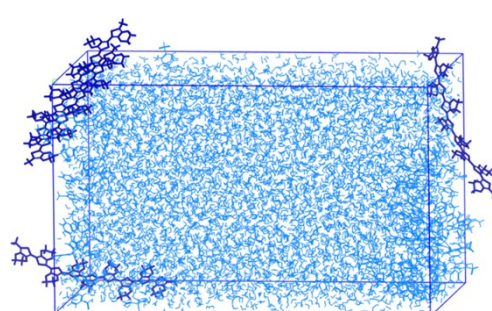
(a) [BnPhIM-*o*OCH₃]⁺:[BF₄]⁻



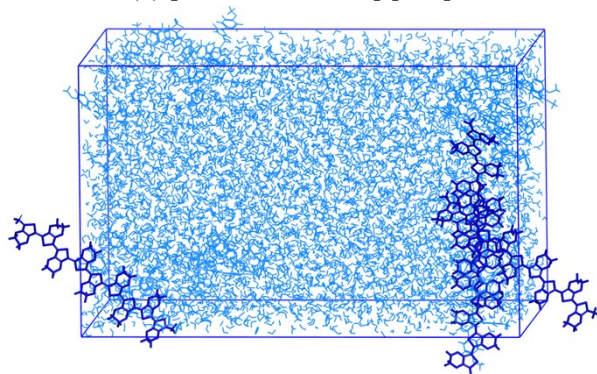
(d) [BnPhIM-*o*OCH₃]⁺:[B(CN)₄]⁻



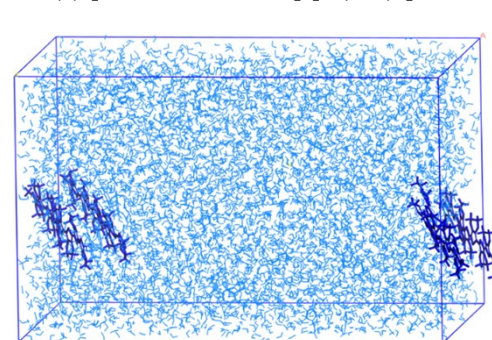
(b) [BnPhIM-*m*OCH₃]⁺:[BF₄]⁻



(e) [BnPhIM-*m*OCH₃]⁺:[B(CN)₄]⁻

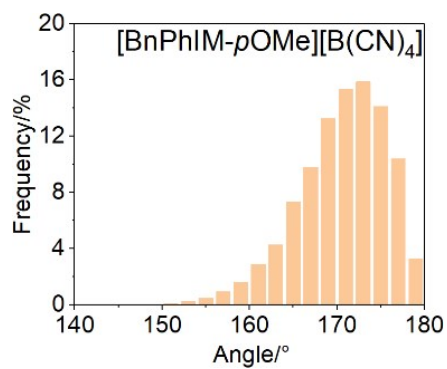


(c) [BnPhIM-*p*OCH₃]⁺:[BF₄]⁻

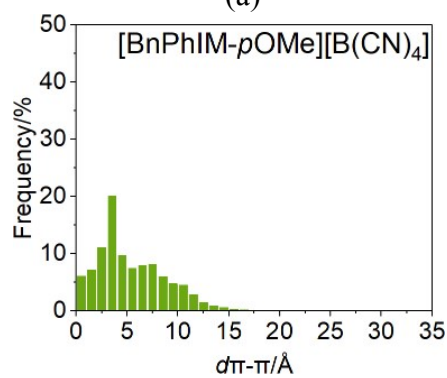


(f) [BnPhIM-*p*OCH₃]⁺:[B(CN)₄]⁻

Fig. S6. The last snapshots of PEDOT in [BnPhIM-*o*OMe]⁺, [BnPhIM-*m*OMe]⁺, and [BnPhIM-*p*OMe]⁺ combined with [BF₄]⁻ and [B(CN)₄]⁻ modified solution.



(a)



(b)

Fig. S7. Histogram of the angle between neighboring thiophene ring in each PEDOT chain (a) and the $d_{\pi-\pi}$ of neighboring PEDOT chains (b) for [BnPhIM-*p*OMe]:[B(CN)₄]-PEDOT system.

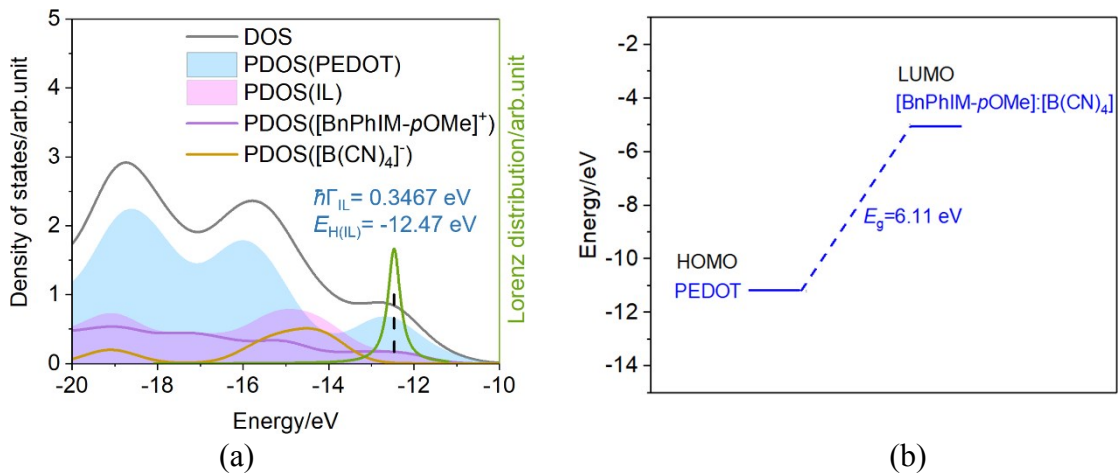


Fig. S8. (a) The density of states and Lorentzian distribution of the HOMO level of [BnPhIM-*p*OMe]:[B(CN)₄] IL. And (b) The HOMO energy level of PEDOT, the LUMO energy level of [BnPhIM-*p*OMe]:[B(CN)₄], and the energy gap between the two orbitals in IL-PEDOT complexes.

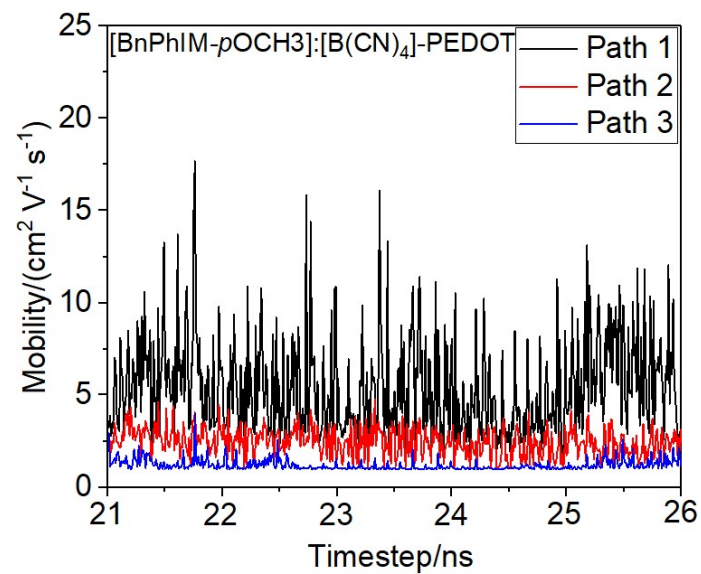


Fig. S9. Dynamic evolution of hole mobility of PEDOT after modulated by [BnPhIM-*p*OCH₃]:[B(CN)₄].

References

1. J. P. Muscat and D. M. Newns, *Prog. Surf. Sci.*, 1978, **9**, 1-43.
2. P. Persson, M. J. Lundqvist, R. Ernstorfer, W. A. Goddard and F. Willig, *J. Chem. Theory. Comput.*, 2006, **2**, 441-451.
3. M. N. Paddon-Row, *Adv. Phys. Org. Chem.* 2003, **38**, 1-85.
4. Z. Shuai, L. Wang and C. Song, *Springer Science & Business Media*, 2012.
5. R. A. Marcus and S. Norman, *BBA-Bioenergetics*, 1985, **811**, 265-322.
6. R. A. Marcus, *Rev. Mod. Phys.*, 1993, **65**, 599.
7. R. A. Marcus, *J. Chem. Phys.*, 1965, **43**, 679-701.
8. L. B. Schein, A R. McGhie, *Phys. Rev. B*, 1979, **20**, 1631-1639.
9. A. de Izarra, S. Park, J. Lee, Y. Lansac and Y. H. Jang, *J. Am. Chem. Soc.*, 2018, **140**, 5375-5384.
10. S. Emamian, T. Lu, H. Kruse and H. Emamian, *J. Comput. Chem.*, 2019, **40**, 2868-2881.